THE JOURNAL OF BIOLOGICAL CHEMISTRY VOL. 290, NO. 30, pp. 18519–18533, July 24, 2015

Differential Regulation of Multiple Steps in Inositol 1,4,5-Trisphosphate Signaling by Protein Kinase C Shapes Hormone-stimulated Ca^{2+} Oscillations*

Received for publication, April 9, 2015, and in revised form, June 3, 2015 Published, JBC Papers in Press, June 15, 2015, DOI 10.1074/jbc.M115.657767

Paula J. Bartlett, Walson Metzger, Lawrence D. Gaspers, and Andrew P. Thomas[1]

From the Department of Pharmacology and Physiology, New Jersey Medical School Rutgers, The State University of New Jersey, Newark, New Jersey 07103

Background: The effects of inositol 1,4,5-trisphosphate (IP_3)-linked hormones are determined by the frequency, amplitude, and duration of Ca^{2+} oscillations.
Results: Comparison of IP_3 uncaging and hormone stimulation showed that PKC has distinct effects on IP_3 formation, metabolism, IP_3 receptor function, and Ca^{2+} wave propagation.
Conclusion: PKC modulates Ca^{2+} oscillation frequency, duration, and wave velocity.
Significance: PKC feedback shapes Ca^{2+} oscillations and provides signal versatility.

How Ca^{2+} oscillations are generated and fine-tuned to yield versatile downstream responses remains to be elucidated. In hepatocytes, G protein-coupled receptor-linked Ca^{2+} oscillations report signal strength via frequency, whereas Ca^{2+} spike amplitude and wave velocity remain constant. IP_3 uncaging also triggers oscillatory Ca^{2+} release, but, in contrast to hormones, Ca^{2+} spike amplitude, width, and wave velocity were dependent on [IP_3] and were not perturbed by phospholipase C (PLC) inhibition. These data indicate that oscillations elicited by IP_3 uncaging are driven by the biphasic regulation of the IP_3 receptor by Ca^{2+}, and, unlike hormone-dependent responses, do not require PLC. Removal of extracellular Ca^{2+} did not perturb Ca^{2+} oscillations elicited by IP_3 uncaging, indicating that reloading of endoplasmic reticulum stores via plasma membrane Ca^{2+} influx does not entrain the signal. Activation and inhibition of PKC attenuated hormone-induced Ca^{2+} oscillations but had no effect on Ca^{2+} increases induced by uncaging IP_3. Importantly, PKC activation and inhibition differentially affected Ca^{2+} spike frequencies and kinetics. PKC activation amplifies negative feedback loops at the level of G protein-coupled receptor PLC activity and/or IP_3 metabolism to attenuate IP_3 levels and suppress the generation of Ca^{2+} oscillations. Inhibition of PKC relieves negative feedback regulation of IP_3 accumulation and, thereby, shifts Ca^{2+} oscillations toward sustained responses or dramatically prolonged spikes. PKC down-regulation attenuates phenylephrine-induced Ca^{2+} wave velocity, whereas responses to IP_3 uncaging are enhanced. The ability to assess Ca^{2+} responses in the absence of PLC activity indicates that IP_3 receptor modulation by PKC regulates Ca^{2+} release and wave velocity.

Calcium oscillations and waves generated by the activation of PLC-linked[2] GPCRs regulate a multitude of mechanisms from gene transcription to secretion (1–3). In many cell types, including hepatocytes, stimulus strength is encoded by the frequency of Ca^{2+} oscillations, with interspike intervals ranging from >250 s at low hormone concentrations to <30 s when challenged with higher hormone levels (1, 4–6). These Ca^{2+} signals are generated by PLC-mediated hydrolysis of phosphatidylinositol bisphosphate (PIP_2) to yield IP_3 and the subsequent activation of IP_3R Ca^{2+} release channels in the ER (7). However, the mechanisms driving the subsequent repetitive Ca^{2+} oscillations have yet to be fully resolved (8–12). Many studies have aimed to determine whether these oscillations arise solely because of the biphasic effects of cytosolic [Ca^{2+}] on IP_3R gating (13–16), *i.e.* Ca^{2+}-induced Ca^{2+} release (CICR), or whetherregenerativePLCactivationand/orcyclicalproteinphosphorylation events are also required (17–19). We have demonstrated recently that intracellular buffering of IP_3, using a recombinant protein containing the ligand binding domain of rat IP_3R type I, results in an inhibition of Ca^{2+} oscillations, a decrease in the rates of Ca^{2+} rise, and a slowing of Ca^{2+} wave propagation speed (17, 20). These data demonstrate that IP_3 levels dynamically regulate Ca^{2+} oscillations, providing evidence that cross-coupling between IP_3 and Ca^{2+} is required to maintain hormone-induced Ca^{2+} oscillations in non-excitable cells such as hepatocytes.

The Ca^{2+} oscillation frequency increases with agonist concentration in hepatocytes (1, 5, 6), but the individual Ca^{2+} spikes have a constant amplitude and rate of rise and propagate as intracellular Ca^{2+} waves at a constant velocity independent of agonist dose. Nevertheless, the falling phase of the [Ca^{2+}] spikes shows greater diversity (1, 6), and different agonists can

* This work was supported, in whole or in part, by National Institutes of Health Grants DK082954 and AI099277 (to A. P. T.). This work was also supported by the Thomas P. Infusion Endowed Chair (to A. P. T.). The authors declare that they have no conflicts of interest with the contents of this article.
[1] To whom correspondence should be addressed: Dept. of Pharmacology and Physiology, New Jersey Medical School Rutgers, The State University of New Jersey, Newark, NJ 07103. Tel.: 973-972-4460; Fax: 973-972-7950; E-mail: andrew.thomas@rutgers.edu.

[2] The abbreviations used are: PLC, phospholipase C; GPCR, G protein-coupled receptor; PIP_2, phosphatidylinositol bisphosphate; IP_3, inositol 1,4,5-trisphosphate; IP_3R, inositol 1,4,5-trisphosphate receptor; ER, endoplasmic reticulum; CICR, Ca^{2+}-induced Ca^{2+} release; CFP, cyan fluorescent protein; YFP, yellow fluorescent protein; PMA, phorbol-12-myristate-13-acetate; BIM, bisindolylmaleimide I; DR, down-regulation; PH, pleckstrin homology.

give characteristically distinct shapes of [Ca^{2+}] spikes that vary only in the decay phase, even when observed in the same individual cell (2, 17, 19, 20). Moreover, the duration of cytosolic Ca^{2+} elevation, in addition to spike frequency, has been demonstrated to regulate transcription (21–23). It is therefore important to determine not only how PLC-dependent Ca^{2+} oscillations are generated but also how spike and wave kinetics are further modulated to account for the versatility of Ca^{2+} signaling.

Long interspike periods between Ca^{2+} transients at low hormone doses and the broad dynamic range of frequency modulation suggest that Ca^{2+} interspike periods and spike kinetics are dynamically controlled by feedback loops that regulate IP_3 generation and metabolism as well as IP_3R function (17, 20). PLC-dependent signal transduction activates PKC (24), which, in turn, has the potential to phosphorylate and regulate multiple proteins in the Ca^{2+} signaling cascade, including GPCRs (25, 26), PLC (27), IP_3R (28, 29), and IP_3 kinase (30). Importantly, concurrent with Ca^{2+} oscillations, repetitive translocation of PKC isoforms, both conventional and novel, to the plasma membrane have been reported (31, 32), indicating cyclic activation of these enzymes. Furthermore, previous studies in hepatocytes have shown that both activation and inhibition of PKC can affect hormone-induced Ca^{2+} oscillation kinetics (33, 34).

In this study, we compared Ca^{2+} signals elicited by hormone and photorelease of caged IP_3 and examined how the ensuing Ca^{2+} oscillations are regulated in response to each stimulus. Our data reveal that Ca^{2+} oscillations elicited by direct release of caged IP_3 are graded, with the transient amplitude, frequency, and wave velocity dependent on the amount of IP_3 released. Moreover, these Ca^{2+} responses were independent of PLC activity, indicating that IP_3 uncaging generates Ca^{2+} oscillations solely through CICR. This is in contrast to hormone-induced Ca^{2+} oscillations, which depend on IP_3 oscillations cross-coupled with Ca^{2+} spiking (17, 20) (*i.e.* regenerative PLC activation) and have characteristic spike properties independent of agonist dose. Therefore, uncaging of IP_3 provides a tool to assess modulators of Ca^{2+} transients in the absence of PLC activity and other hormone-dependent signaling cascades. We show that Ca^{2+} oscillations elicited by IP_3 uncaging persist in the absence of extracellular Ca^{2+}, demonstrating that reloading of ER Ca^{2+} stores does not entrain these periodic Ca^{2+} signals. Modulation of Ca^{2+} signaling by PKC was assessed in both PLC- and CICR-dependent paradigms. Paradoxically, both activation and inhibition of PKC decreased the frequency of hormone-induced Ca^{2+} oscillations but via different mechanisms. Activation of PKC inhibited regenerative IP_3 generation by the GPCR/PLC, whereas inhibition of PKC relieved this negative feedback, allowing more prolonged and sustained IP_3 generation and, therefore, Ca^{2+} release. By contrast, CICR oscillations elicited by uncaging IP_3 were potentiated by PKC activation. Furthermore, PKC down-regulation decreased Ca^{2+} wave velocity in agonist-stimulated cells, whereas it actually increased Ca^{2+} wave velocity after direct IP_3 release. These data demonstrate that PKC activity regulates IP_3 levels via effects on GPCR coupling, PLC activity, and/or IP_3 metabolism while also effecting IP_3R sensitivity to regulate Ca^{2+} spike frequency, width, and Ca^{2+} wave velocity.

Experimental Procedures

Primary Cell Culture—Isolated hepatocytes were prepared by collagenase perfusion of livers obtained from male Sprague-Dawley rats. Cells were maintained in Williams E medium for 2–6 h for experiments using freshly isolated cells or 16–24 h for experiments using overnight cultured cells, as described previously (1, 4). Animal studies were approved by the Institutional Animal Care and Use Committee at Rutgers, New Jersey Medical School.

Cytosolic Ca^{2+} Measurements in Response to Hormones—Calcium imaging experiments were performed in HEPES-buffered physiological saline solution comprised of 25 mM HEPES (pH 7.4), 121 mM NaCl, 5 mM $NaHCO_3$, 10 mM glucose, 4.7 mM KCl, 1.2 mM KH_2PO_4, 1.2 mM $MgSO_4$, 2.0 mM $CaCl_2$, and 0.25% (w/v) fatty acid-free BSA and supplemented with the organic anion transport inhibitors sulfobromophthalein (100 μM) or probenecid (200 μM). Hepatocytes were loaded with Fura-2 by incubation with 2–5 μM Fura-2/AM and Pluronic acid® F-127 (0.02% v/v) for 20–40 min. Cells were transferred to a thermostatically regulated microscope chamber (37 °C). Fura-2 fluorescence images (excitation, 340 and 380 nm, emission 420–600 nm) were acquired at 1.5- to 3-s intervals with a cooled charge-coupled device camera coupled to an epifluorescent microscope, as described previously (35).

Hormone-induced PLC Activity and IP_3 Detection—Intracellular IP_3 levels or PLC activity were measured using FRET-based genetically engineered probes. Isolated hepatocytes were transfected by electroporation with the Amaxa rat/mouse hepatocyte nucleofector kit according to the instructions of the manufacturer (Lonza). PLC activity was determined by cotransfection with $PLC_{\delta4}$YFP and $PLC_{\delta4}$CFPPH domains (cDNA was a gift from Dr. Balla, National Institutes of Health), which yield a FRET signal while bound to membrane PIP_2 that declines as PIP_2 is hydrolyzed. IP_3 measurements were determined with the IP_3 sensor IRIS-1. IRIS-1 cDNA was a gift from Dr. Mikoshiba (RIKEN Brain Science Institute, Japan) (36). FRET images were acquired at 3-s intervals by illumination with 436 ± 20 nm using a 455-nm-long band pass dichroic filter. FRET donor and acceptor fluorescence images were separated with a 505-nm-long band pass dichroic mirror and directed to 480 ± 30 nm (CFP) or 535 ± 40 nm (YFP/Venus) emission filters using an image beamsplitter (Optical Insights™). The FRET ratio was calculated on a cell-by-cell basis and averaged from all expressing cells in the microscope field. FRET signal changes between $PLC_{\delta4}$YFP and $PLC_{\delta4}$CFP PH domains were corrected for YFP bleach using linear regression analysis.

Photorelease of Caged IP_3—Overnight cultured hepatocytes were loaded in HEPES-buffered physiological saline solution with the membrane-permeant form of caged IP_3 (2 μM; D-2, 3-*O*-isopropylidene-6-*O*-(2-nitro-4,5-dimethoxy)benzyl-*myo*-inositol 1,4,5-trisphosphate-hexakis(propionoxymethyl) ester; Sichem GmbH) for 45 min at room temperature, followed by 30-min loading with the calcium indicator dye Fluo-4/AM (5 μM). Cells were transferred to the microscope chamber of a

spinning disc confocal microscope. Fluo-4 images (excitation, 488 nm; emission, 510-nm-long band pass filter) were acquired at 10 Hz. Photorelease of caged IP_3 was achieved by light pulses from a nitrogen-charged UV laser (Photon Technology International). The cell-permeant caged IP_3 is synthesized with the 2- and 3-hydroxyl groups of myo-inositol protected by an isopropylidene group to ensure that the phosphate groups remain in the 1,4 and 5 positions (37). Of note, when released from the cage, this modified form of IP_3 is metabolized at a slower rate, in the order of minutes, compared with natural IP_3, which is metabolized in seconds (37). Cell viability was assessed by the addition of maximal hormone concentrations at the end of each experiment. Only cells responsive to hormone stimulation are included in the presented data.

Western Blotting—Hepatocyte lysates were prepared in a buffer comprised of 150 mM NaCl, 10 mM Tris-HCl, 1 mM EDTA, and 0.2 mM PMSF supplemented with 1% (w/v) SDS, 0.5% (v/v) Nonidet P-40, 10 μg/ml aprotinin, and 1 μg/ml leupeptin (pH 7.4). Lysates were resolved by SDS-PAGE on a 10% polyacrylamide gel and transferred to a PVDF membrane. Membranes were blocked for 1 h in Tris-buffered saline (pH 7.5) containing 5% (w/v) nonfat dry milk and 0.1% (v/v) Tween 20. The membranes were incubated with anti-PKCα, (Cell Signaling Technology), anti-PKCϵ, and anti-PKCζ (Santa Cruz Biotechnology) overnight at 4 °C. The protein loading control was determined by stripping PVDF membranes and reprobing with anti-α-tubulin (Cell Signaling Technology).

[^{3}H]Inositol Phosphate Accumulation—Total [^{3}H]inositol phosphate accumulation was determined as described previously (31). In brief, primary hepatocytes were labeled overnight with 2.5 μCi ml^{-1} *myo*-[^{3}H]inositol (American Radiolabeled Chemicals, Inc.) in 6-well plates. In some studies, cultures were treated overnight with phorbol-12-myristate-13-acetate (PMA) or 4α-PMA (1 μM) to assess the effect of down-regulating PKC. Cultures were washed with HEPES-buffered physiological saline solution and incubated for 20 min at 37 °C, followed by an additional 10-min treatment with 10 mM LiCl to block inositol monophosphatase activity. Cells were treated with 100 nM vasopressin for 15 min in the absence or presence of PMA (1 nM) or bisindolylmaleimide I (BIM, 5 μM) to assess the acute effects of PKC activation and inhibition, respectively. Incubations were terminated by addition of ice-cold tricholoroacetic acid. Water soluble [H^3]inositol-containing components were extracted by addition of tri-*n*-octylamine:1,1,2-trichlorofluoroethane (1:1 ratio). [H^3]inositol phosphates were separated by ion exchange chromatography using Dowex resin in the formate form. Lower-order inositols and glycerophospholipids were removed by elution with 0.4 M ammonium formate/0.1 M formic acid. IP_3 and higher-order inositols were then eluted with 1.2 M ammonium formate/0.1 M formic acid. Ultima-Flo (PerkinElmer Life Sciences) was added to the eluate, and disintegrations per minute was determined using liquid scintillation counting. Data are expressed as a -fold increase over basal (inositol phosphate turnover levels in the absence of hormone).

Data Analysis—Image analysis was performed using in-house customized software and ImageJ (National Institutes of Health). Graph plotting and data analysis were performed with GraphPad Prism software. Statistical analysis was performed using Student's *t* test or one-way analysis of variance where indicated.

Results

Photorelease of Caged IP_3 Elicits Ca^{2+} Oscillations in Hepatocytes—Photorelease of caged IP_3 in hepatocytes induced cytosolic Ca^{2+} increases, with Ca^{2+} oscillations observed in many cells (Fig. 1*A*). Similar to hormone-induced Ca^{2+} oscillations (1, 9), the frequency and number of cells responding to IP_3 uncaging increased with stimulus strength, as determined by the number of UV flashes, and tended toward sustained Ca^{2+} increases with the strongest stimulation (Fig. 1, *B* and *C*). A single pulse from the UV laser resulted in Ca^{2+} responses in only 22.5 ± 10.2% of cells. Incrementally increasing the number of UV flashes (applied as a rapid burst) increased the percentage of cells responding (2× UV, 44.2 ± 14.8%; 3× UV, 84 ± 9.2%; 4× UV, 86.7 ± 8.6%; mean ± S.E. from >100 cells in three independent experiments). In addition, increasing the number of UV flashes shifted the Ca^{2+} signature from predominantly no response and single Ca^{2+} transients at low illumination toward oscillatory and sustained (peak/plateau) Ca^{2+} increases at higher illumination, presumably reflecting increased levels of IP_3 (Fig. 1*C*). Therefore, the Ca^{2+} signals induced by uncaging IP_3 appear to mimic hormone-induced Ca^{2+} responses, the proportion of responsive cells, and the oscillatory and saturated Ca^{2+} responses increasing with stimulus strength.

A characteristic of hormone-induced Ca^{2+} oscillations is that although the frequency increases with agonist dose, Ca^{2+} spike kinetics, including amplitude, rate of rise, and peak width are constant for all agonist doses (1, 5, 6, 9). By contrast, photorelease of caged IP_3 resulted in Ca^{2+} peak heights and widths that increased with stimulus strength (Fig. 1, *D* and *E*). These data are the mean ± S.E. calculated from the average of the first three Ca^{2+} transients from cells in which oscillations were observed at each level of UV exposure. Of particular note, the mean duration of Ca^{2+} spikes elicited by a single UV flash was 3.8 ± 0.24 s at half-peak height, which is much shorter than hormone-stimulated Ca^{2+} transients measured in this work (Figs. 4 and 7) and previous studies (1, 38). Broader Ca^{2+} spike widths were achieved with multiple UV flashes (11.5 ± 2.2 s at half-peak height for 3× UV flashes), but this is still a shorter duration than the Ca^{2+} spike widths of >20 s typically observed with hormone stimulation. The velocity of Ca^{2+} waves elicited by IP_3 uncaging was also dependent on the number of UV flashes (Fig. 1*F*). Ca^{2+} waves induced by hormones propagate at 15–25 μm/s independent of hormone dose (5), whereas Ca^{2+} waves induced by IP_3 uncaging rose from 8.2 μm/s ± 0.7 at 1× UV to 23.9 μm/s ± 4.8 with 3× UV.

IP_3-induced Ca^{2+} Oscillations Do Not Require PLC Activity—To address whether IP_3 regeneration through Ca^{2+} activation of PLC is required to elicit Ca^{2+} oscillations in response to photolysis of IP_3, we performed experiments in the presence of the aminosteroid PLC inhibitor U71322. Hepatocytes were loaded with caged IP_3 and concurrently treated for 75 min with 20 μM U73122, the inactive analogue U73433, or vehicle

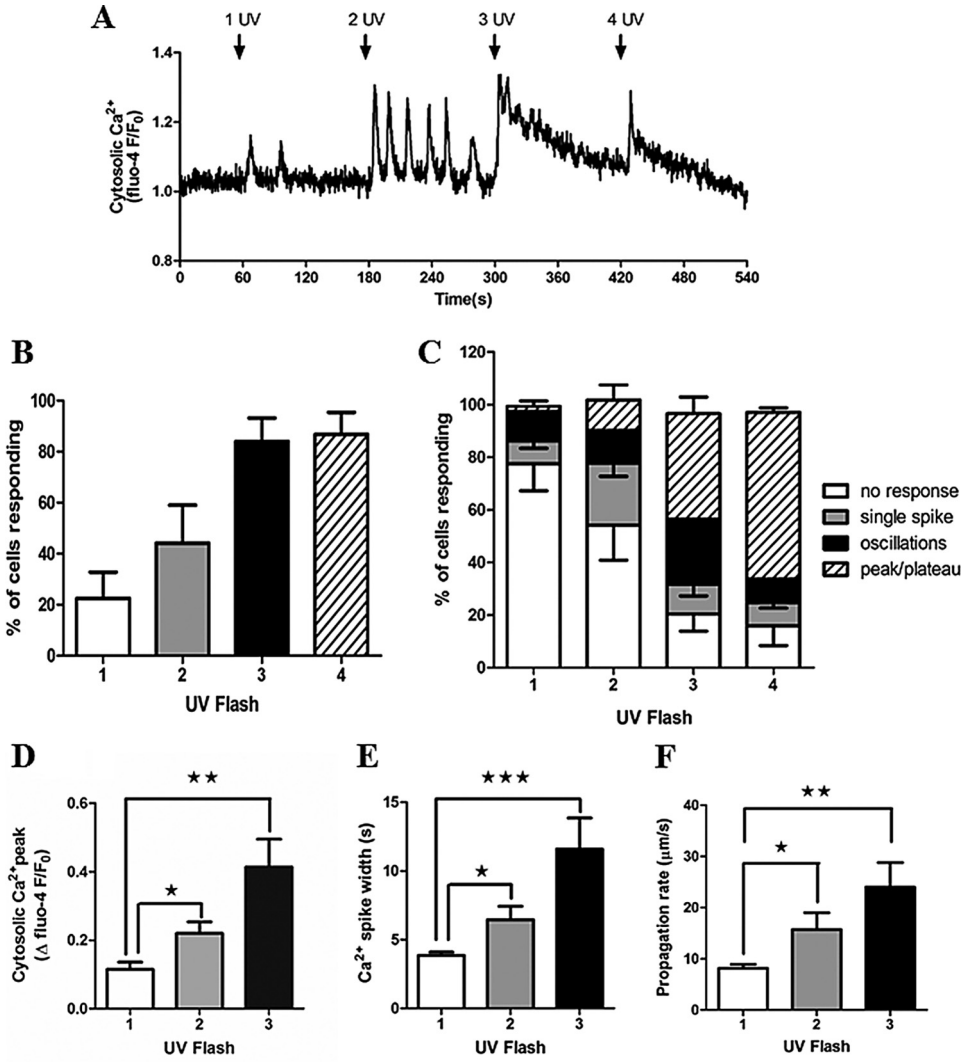

FIGURE 1. **Photorelease of caged IP_3 elicits Ca^{2+} oscillations in primary rat hepatocytes.** Isolated hepatocytes were cultured overnight and then loaded with caged IP_3 and Fluo-4. *A*, representative trace showing cytosolic Ca^{2+} responses to photolysis of caged IP_3. Rapid trains of one, two, three, or four UV pulses were applied as indicated (*arrows*). *B*, the percentage of cells responding to one to four UV flash events. *C*, comparison of the types of Ca^{2+} responses observed after each train of UV pulses: no response, single spike, oscillations, or a sustained Ca^{2+} increase (peak/plateau). Data shown are mean ± S.E. from ≥100 cells from five independent experiments. *D* and *E*, summary of Ca^{2+} transient amplitude (*D*) and Ca^{2+} spike width measured at half-peak height (*E*) in cells in which oscillations were observed after one, two, and three UV flashes. Data are mean ± S.E. of the first three Ca^{2+} transients for each individual cell ($n = 15$). *F*, Ca^{2+} wave propagation rates as a function of number of UV flashes. Data are mean ± S.E. from cells in which Ca^{2+} waves were observed after one, two, and three UV flashes ($n = 13$). *, $p < 0.05$; **, $p < 0.01$; ***, $p < 0.001$; Student's *t* test.

(dimethyl sulfoxide). The cells were first exposed to a rapid train of 4× UV flashes to uncage IP_3, followed by 10 nM vasopressin (Fig. 2, *A* and *B*). The percentage of cells eliciting a Ca^{2+} increase and oscillatory Ca^{2+} responses to each stimulus are summarized in Fig. 2, *C* and *D*. In our hands, non-toxic concentrations of U73122 were insufficient to completely block hormone-induced Ca^{2+} increases in all cells (higher concentrations perturbed Ca^{2+} release by thapsigargin, indicating off-target effects). Nevertheless, a significant inhibition of vasopressin-induced Ca^{2+} transients was observed after U73122 treatment. U73122 reduced the percentage of cells responding to hormone stimulation from 81 ± 6 to 33 ± 9 and the percentage of cells displaying Ca^{2+} oscillations from 60 ± 5 to 22 ± 6. By contrast, the Ca^{2+} increases and oscillatory responses elicited by photolysis of caged IP_3 were not significantly different between treatment groups (Fig. 2, *C* and *D*).

We also considered the possibility that ATP released from the hepatocytes in culture might act in a paracrine fashion to cause tonic subthreshold activation of PLC, the activity of which could be amplified upon direct photorelease of IP_3. Pretreatment of hepatocytes with 30 units/ml (5 min) of apyrase to hydrolyze extracellular ATP was without effect on the number of cells responding to photolysis of caged IP_3 or the proportion of cells displaying oscillatory changes in cytosolic Ca^{2+} (Fig. 2, *E* and *F*). Taken together, these data indicate that positive feedback of Ca^{2+} on PLC does not contribute to the Ca^{2+} signals elicited by uncaging IP_3, and, when IP_3 is sufficiently elevated, Ca^{2+} oscillations are driven primarily by CICR at the IP_3R.

Plasma Membrane Ca^{2+} Entry Is Not a Requirement for IP_3-driven Ca^{2+} Oscillations—Store-operated Ca^{2+} entry plays a fundamental role in maintaining Ca^{2+} homeostasis and to

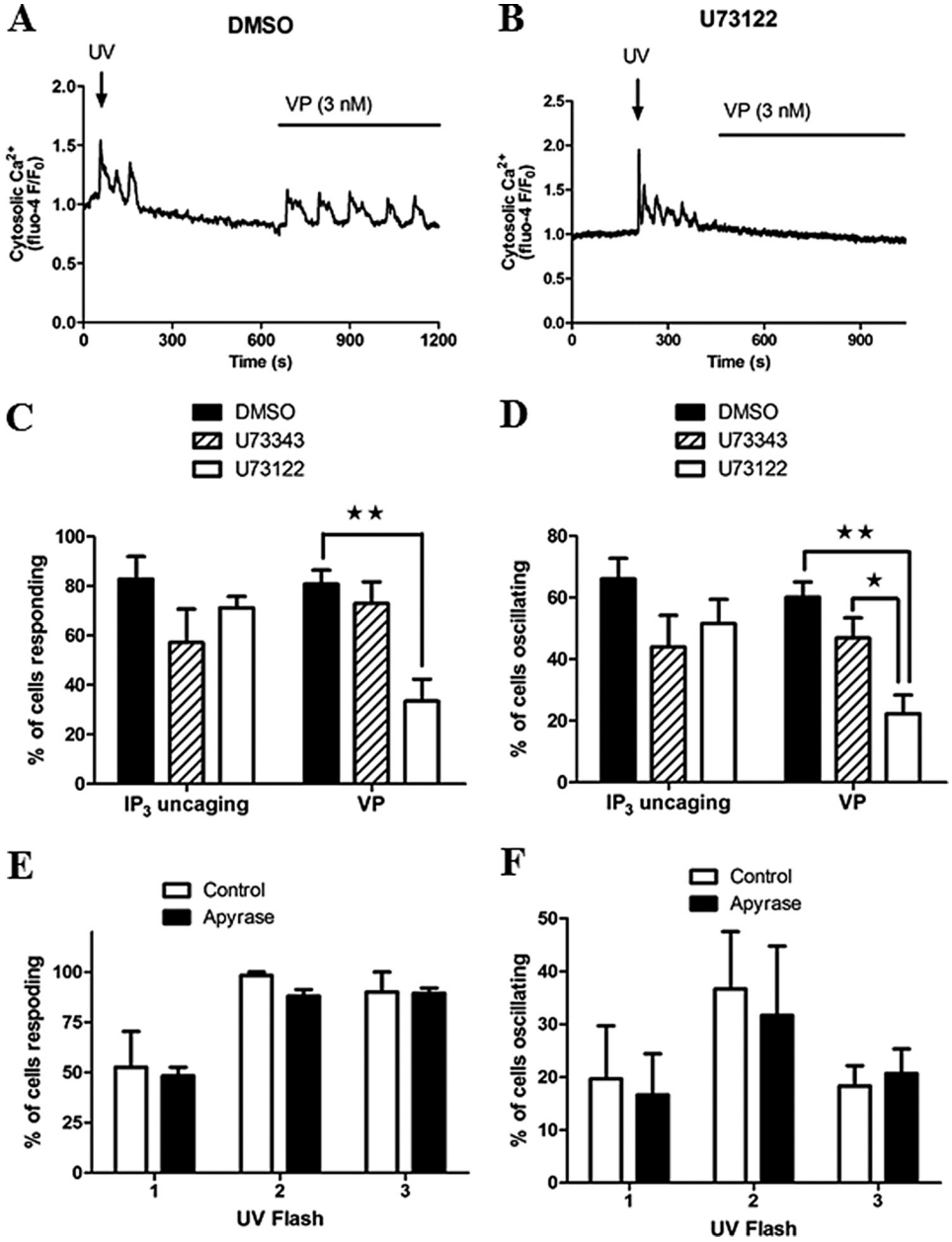

FIGURE 2. **IP_3-induced Ca^{2+} oscillations do not depend upon the activation of PLC.** Hepatocytes cultured overnight and loaded with caged IP_3 and Fluo-4 were treated with the PLC inhibitor U73122, the inactive analogue U74344 (20 μM for each drug, 75 min), or vehicle (dimethyl sulfoxide (*DMSO*), 0.1% v/v). Cells were then stimulated with UV illumination followed by 3 nM vasopressin (*VP*) as indicated. *A* and *B*, representative Ca^{2+} responses in dimethyl sulfoxide-treated (*A*) or U73122-treated (*B*) cells are shown. *C* and *D*, the effect of PLC inhibition on the percentage of responsive (*C*) and oscillating cells (*D*) to each stimulus are summarized. Data are representative of ≥60 cells from four independent experiments. *E* and *F*, summary of the effect of apyrase (30 units/ml, 5 min) on the proportion of cells responding (*E*) or the percentage of cells giving oscillatory Ca^{2+} responses (*F*). Data are mean ± S.E. of 45 cells from three independent experiments. *, $p < 0.05$; **, $p < 0.01$; Student's *t* test.

replete internal Ca^{2+} stores when cells respond to Ca^{2+}-mobilizing hormones (39). However, there is a continuing debate regarding the importance of store-operated Ca^{2+} entry and Ca^{2+} store load in the generation and feedback control of hormone-stimulated Ca^{2+} oscillations (40–42). To determine whether extracellular Ca^{2+} entry regulates IP_3R activation or sensitivity to IP_3, we assessed Ca^{2+} signals elicited by photorelease of caged IP_3 in the absence and presence of extracellular Ca^{2+}. Hepatocytes were maintained in either HEPES-buffered physiological saline solution containing 2 mM $CaCl_2$ or switched to Ca^{2+}-free buffer 5–10 min prior to uncaging IP_3 with 3× UV flashes (Fig. 3). A somewhat higher proportion of cells did not respond to photorelease of caged IP_3 in Ca^{2+}-free (37.3 ± 0.7%) compared with Ca^{2+}-replete conditions (19.3 ± 3.1%) (Fig. 3*C*), which may reflect an effect of partial Ca^{2+} store depletion. Nevertheless, Ca^{2+} oscillations were still observed in response to IP_3 uncaging in the presence or absence of extracellular Ca^{2+} (Fig. 3, *A* and *B*), with no impact on oscillation frequency over a 5-min period (Fig. 3*D*). These data indicate that plasma membrane Ca^{2+} entry is not a requirement to sustain repetitive Ca^{2+} release from the ER. However, the width of the Ca^{2+} spike, measured at half-peak height for the first three

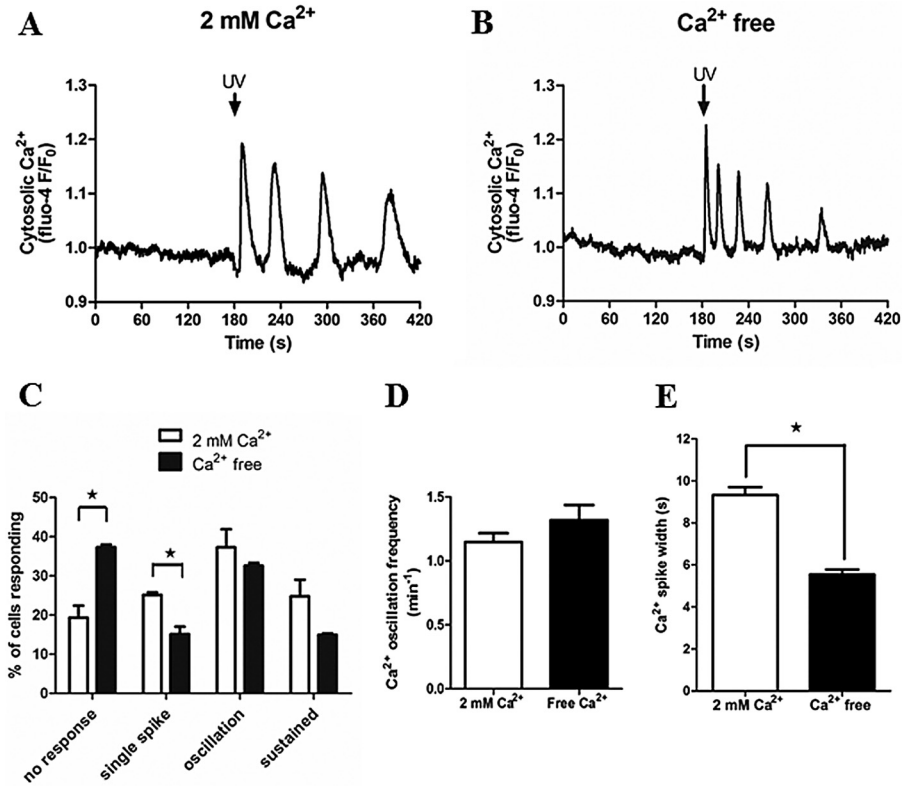

FIGURE 3. **Extracellular Ca^{2+} is not required for IP_3-induced Ca^{2+} oscillations.** Isolated hepatocytes loaded with caged IP_3 and Fluo-4 were stimulated with 3 UV flashes (*UV*). *A* and *B*, representative traces of Ca^{2+} responses are shown in the presence (*A*) and absence (*B*) of extracellular Ca^{2+}. *C–E*, summary of the Ca^{2+} signatures observed (*C*), oscillation frequency (*D*), and Ca^{2+} peak width at half-height (*E*) in the presence and absence of extracellular Ca^{2+}. Data are mean ± S.E. of 25 cells from two independent experiments. *, $p < 0.05$, Student's *t* test.

Ca^{2+} transients, was decreased significantly in the absence of extracellular Ca^{2+} (5.5 ± 0.2 s compared with 9.3 ± 0.4 s in the presence of extracellular Ca^{2+}). Therefore, Ca^{2+} entry and ER Ca^{2+} load may contribute to IP_3R-induced Ca^{2+} transients by prolonging spike duration (Fig. 3*E*).

PKC Down-regulation Perturbs Negative Feedback Inhibition of Ca^{2+} Mobilization—Previous studies have highlighted the complexity of PKC regulation of hormone-induced Ca^{2+} oscillations in hepatocytes, reporting that both activators and inhibitors of PKC suppressed the responses to phenylephrine (33, 34). We examined the effect of chronic down-regulation of conventional and novel PKCs (PKC-DR) by overnight treatment (16–24 h) with 1 μM PMA or the inactive analogue 4α-PMA. A comparison of responses in control 4α-PMA-treated and PMA-treated hepatocytes revealed a dramatic shift in the type of Ca^{2+} responses elicited by phenylephrine (20 μM). Under control conditions, 65 ± 6.5% of cells responded with an oscillatory Ca^{2+} signature (Fig. 4*A* shows a representative trace of a Ca^{2+} response in control cells), whereas PKC-DR resulted in predominately sustained Ca^{2+} rises in 73 ± 3% of cells (see Fig. 4*B* for a representative trace) compared with only 11 ± 0.6% of sustained responses in control cells. In PKC-DR cells, only 16.2 ± 2.2% responded with oscillatory Ca^{2+} signatures (Fig. 4*C* shows a representative trace of Ca^{2+} oscillations after PKC-DR). The proportion of cells responding with oscillatory or sustained responses for each treatment group is summarized in Fig. 4*D*. The small population of PKC-DR cells in which Ca^{2+} oscillations were observed displayed responses characteristically different from the stereotypic Ca^{2+} oscillations in control cells. The oscillation frequency was reduced, and the spike widths were very substantially prolonged. The individual Ca^{2+} spike widths measured at half-peak height in phenylephrine-stimulated control cells were very consistent, with a mean value of 24 ± 0.6 s, whereas the spike durations in PKC-DR cells were almost 3-fold longer, with a width at half-peak height of 68 ± 3.3 s (Fig. 4*E*). We confirmed by Western blotting that treating cells overnight with phorbol ester leads to the down-regulation and degradation of the conventional, PKCα, and novel PKCϵ (phorbol ester-activated PKC isoenzymes in hepatocytes) without affecting the atypical isoform PKCζ1 (Fig. 4*F*).

PKC phosphorylation of the plasma membrane Ca^{2+} pump and of Orai channels has been reported (43, 44), indicating that PKC activity may regulate plasma membrane Ca^{2+} efflux and/or entry. Indeed, Orai1 has been shown to be basally phosphorylated by PKC, and inhibition of PKC leads to enhanced Ca^{2+} entry (44). To determine whether PKC-DR affects Ca^{2+} transport across the plasma membrane in hepatocytes, we measured Ca^{2+} influx and efflux rates in cells treated overnight with PMA or 4α-PMA (Fig. 5). ER Ca^{2+} stores were depleted with thapsigargin (Fig. 5, *A–C*) or ATP (to assess agonist-dependent effects on Ca^{2+} influx) (Fig. 5, *D--F*) in the absence of extracellular Ca^{2+} to induce Store-operated Ca^{2+} entry pathways. The PKC-DR protocol did not affect the rates of Ca^{2+} influx upon Ca^{2+} readdition (Fig. 5, *B* and *E*) or the rates of plasma membrane Ca^{2+} pump-mediated Ca^{2+} efflux from the cells after removal of extracellular Ca^{2+} (Fig. 5, *C* and *F*). These data

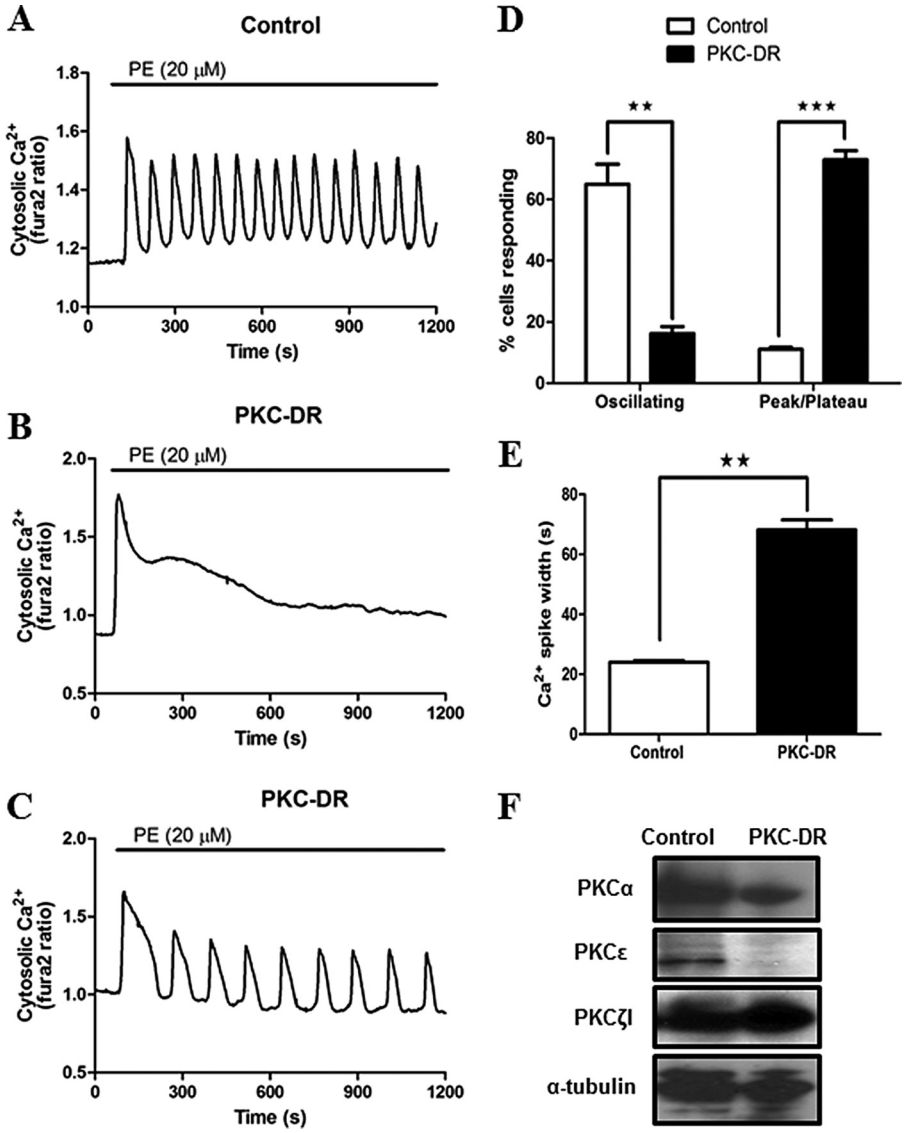

FIGURE 4. **Down-regulation of PKC enhances hormone-stimulated Ca^{2+} signals in cultured hepatocytes.** Cultured hepatocytes were treated overnight with the inactive analogue 4α-PMA (1 μM, *control*) or PMA (1 μM, *PKC-DR*) to down-regulate classical and novel PKC isoforms. Cells were loaded with Fura-2 and then stimulated with phenylephrine (*PE*, 20 μM). *A*—*C*, typical agonist-induced Ca^{2+} responses are shown for control (*A*) and PKC-DR (*B* and *C*) cells. *D* and *E*, summary data showing the effects of PKC down-regulation on the type of Ca^{2+} responses and the width of the Ca^{2+} spikes induced by PE stimulation. Data are mean ± S.E. from ≥50 cells from three independent experiments. **, $p < 0.01$; ***, $p < 0.001$; Student's *t* test. *F*, Western blots showing PKCα, PKCε, and PKCζ protein levels in control and PKC-DR hepatocyte lysates. Levels of α-tubulin are shown as loading controls.

suggest that PKC activity does not play a major role in regulating Ca^{2+} entry or Ca^{2+} extrusion at the plasma membrane in hepatocytes.

Negative feedback regulation by PKC on both GPCRs and PLC isoenzymes has been implicated in the regulation of Ca^{2+} oscillations (27, 31, 45). Therefore, we assessed the effect of PKC-DR on hormone-stimulated PLC activity and IP_3 generation in hepatocytes using FRET-based molecular indicators. To monitor PLC activity, CFP and YFP proteins conjugated to PLCδ4PH domain were coexpressed. Hormone-stimulated PIP_2 breakdown leads to a decrease in FRET between the CFP and YFP moieties, as described previously for CFP and YFP PLCδ1PH (46). The pleckstrin homology (PH) domain of PLCδ4 has a lower affinity for IP_3 compared with PLCδ1, providing a more selective readout of PLC activity (PIP_2 hydrolysis) over intracellular [IP_3]. Dynamic changes in cytosolic [IP_3] were determined with the IRIS-1 molecular probe containing a mutated version of the ligand binding domain of IP_3R type 1 flanked by CFP and Venus (20, 36). PLC activity elicited by agonist stimulation (ATP, 200 μM) was potentiated in PKC-DR cells more than 2-fold compared with control 4α-PMA-treated cells (Fig. 6*A*). Similar effects on ATP-induced IP_3 increases were also observed (Fig. 6*B*). Therefore, loss of PKC enhances PLC activity and increases the overall level of cellular [IP_3], resulting in sustained and prolonged Ca^{2+} responses. These data indicate that negative feedback inhibition of IP_3 generation by PKC is a key element in shaping agonist-induced Ca^{2+} oscillations.

Acute Effect of PKC Activation and Inhibition on Hormone-evoked Ca^{2+} Signaling—In view of results with PKC-DR, we investigated the effects of acute activation or inhibition of PKC on Ca^{2+} signals evoked by hormone. Hepatocytes were treated

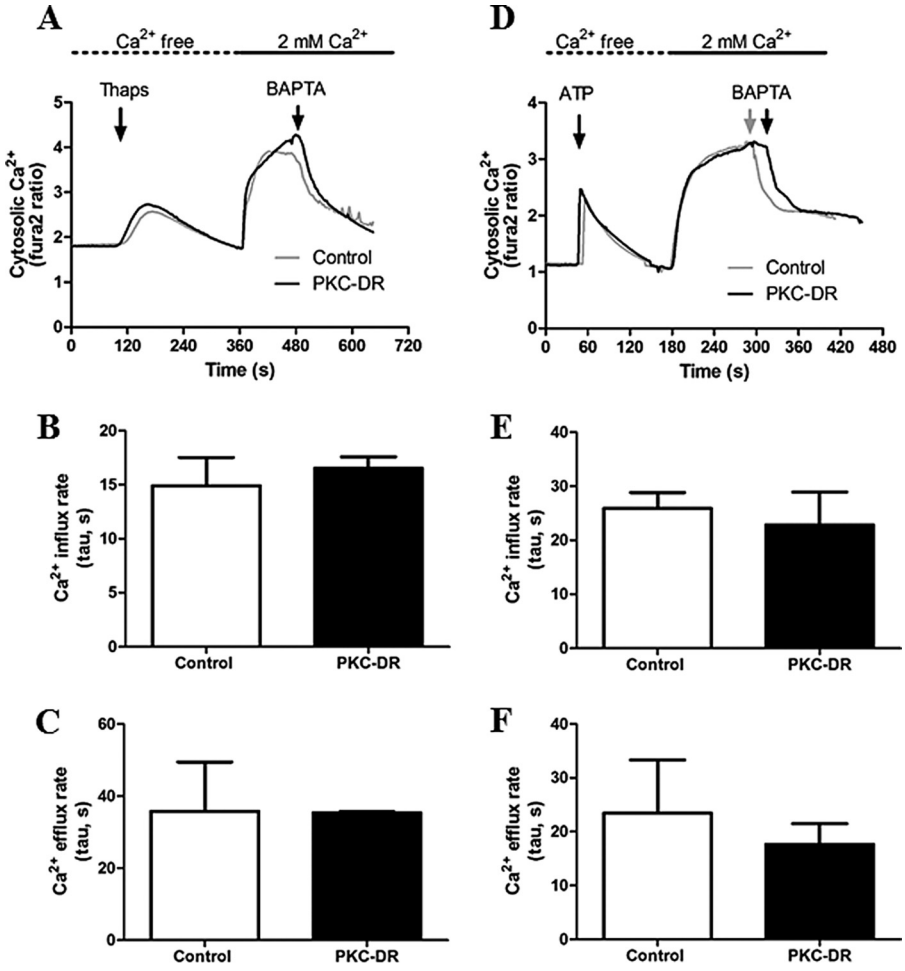

FIGURE 5. **Measurement of Ca^{2+} influx and efflux rates in control and PKC-DR hepatocytes.** Hepatocytes were treated overnight with 4α-PMA (1 μM, *Control*) or PMA (1 μM, *PKC-DR*) and then loaded with Fura-2. Cultures were washed into Ca^{2+}-free buffer prior to data acquisition. *A*—*F*, internal Ca^{2+} stores were depleted with thapsigargin (*Thaps*, 4 μM) (*A–C*) or by stimulation with the purinergic agonist ATP (200 μM) (*D–F*), followed by repletion of extracellular Ca^{2+} (2 mM) to initiate Ca^{2+} entry. Where indicated, the buffer was switch to Ca^{2+}-free medium plus 5 mM BAPTA to stop Ca^{2+} influx and measure the rates of Ca^{2+} efflux from the cell. Ca^{2+} influx (*B* and *E*) and efflux (*C* and *F*) were plotted, and exponential rate constants (*tau*) were calculated using non-linear regression analysis. Similar results were obtained when the initial rates were measured (data not shown).

with phenylephrine at a dose that elicited repetitive Ca^{2+} oscillations (1–20 μM), and then the acute effects of PMA (1 nM) or BIM (5 μM) on the Ca^{2+} response was determined in each cell. Changes in Ca^{2+} oscillation frequency and Ca^{2+} spike width were calculated in hepatocytes that displayed continuous Ca^{2+} spiking for at least 5 min after application of drugs. Activation of PKC by PMA caused either a decrease in oscillation frequency (Fig. 7*A*, *top panel*) or a halt in oscillations (Fig. 7*A*, *bottom panel*). PMA treatment reduced the oscillation frequency in 32 ± 5% of the cell population and terminated the response in the remaining 68 ± 5%. This negative regulatory effect of PKC activation is consistent with the enhanced PLC/IP_3 and Ca^{2+} responses observed in PKC-DR cells described above. However, counterintuitively, inhibition of PKC with BIM also decreased Ca^{2+} oscillation frequency. Following BIM treatment, the Ca^{2+} oscillation frequency was reduced in a majority of cells (63 ± 11% of cells, Fig. 7*B*, *top panel*), and there was a complete loss of Ca^{2+} oscillations in a smaller proportion of cells (37 ± 11% of cells, Fig. 7*B*, *bottom panel*).

Although the effects of PMA and BIM on the frequency of agonist-induced Ca^{2+} oscillations both manifest as frequency decreases, there were quantitative and qualitative differences in the responses to activation and inhibition of PKC with these agents. PMA treatment caused a 50% reduction in oscillation frequency (Fig. 7*C*) but only a small change in spike width (Fig. 7*D*). By contrast, BIM caused a modest 20% reduction in Ca^{2+} oscillation frequency (Fig. 7*C*) but dramatically prolonged the duration of the Ca^{2+} spikes (Fig. 7*D*). Furthermore, comparison of the effects of PMA and BIM revealed qualitative differences with respect to the termination of the Ca^{2+} oscillations. PKC activation with PMA caused an abrupt termination of the response or one to three blunted Ca^{2+} spikes prior to cessation, as shown in Fig. 7*A*, *bottom panel*. The termination of Ca^{2+} oscillations following PKC inhibition with BIM was quite different. There was a final sustained or peak/plateau Ca^{2+} increase (Fig. 7*B*) similar to those typically observed with a maximum hormone dose (1, 47, 48). Therefore, the effects of PKC inhibition with BIM are compatible with the enhanced Ca^{2+} signaling observed with PKC-DR. There is a broadening of the Ca^{2+} oscillations and shift from oscillatory to sustained Ca^{2+} signals (compare Fig. 7*B* with Fig. 4). Moreover, the apparent reduction in Ca^{2+} oscillation frequency with BIM can

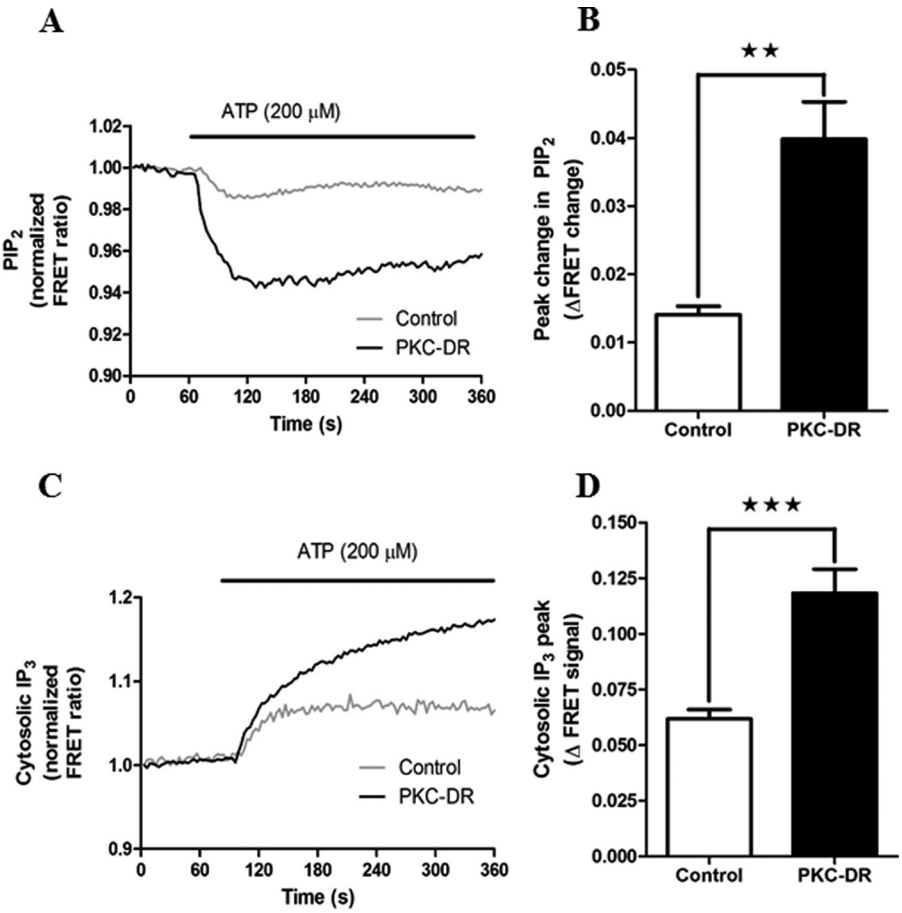

FIGURE 6. **Down-regulation of PKC potentiates hormone-stimulated PLC activity and IP_3 levels.** Hepatocytes were transfected with eCFP-PH-PLCδ4 and eYFP-PH-PLCδ4 to monitor PIP_2 levels (PLC activity) or IRIS-1 to monitor IP_3 production (see "Experimental Procedures") and then cultured overnight in the presence of 2 μM 4α-PMA (*Control*) or 2 μM PMA (*PKC-DR*). Cells were stimulated with ATP (200 μM), and maximal FRET changes were determined. *A*, representative traces showing the mean PLC response in control and PKC-DR cells. Traces are averaged from 27 and 25 cells, respectively, and are normalized to the basal FRET level (mean basal FRET values were 0.85 ± 0.011 for control and 1.028 ± 0.066 for PKC-DR cells, $p = 0.033$, Student's *t* test). *B*, mean peak FRET change (absolute values) ± S.E. for ≥70 cells from five independent experiments. **, $p < 0.01$, Student's *t* test. *C*, representative experiment showing the effect of PKC down-regulation on ATP-induced increases in IP_3 levels for control and PKC-DR cells. Traces are averaged from five and four cells, respectively, and are normalized to the basal FRET level (mean basal FRET values were 0.66 ± 0.016 for control and 0.70 ± 0.013 for PKC-DR cells, $p = 0.053$, Student's *t* test). *D*, mean peak FRET change (absolute values) ± S.E. for ≥25 cells from 10 independent experiments. ***, $p < 0.001$, Student's *t* test.

be ascribed to the prolongation of the Ca^{2+} spike widths because the interspike interval actually decreased from 56.7 ± 5.7 s to 39.6 ± 4.6 s ($p < 0.01$) after BIM addition. The decreased Ca^{2+} oscillation frequency and complete termination of Ca^{2+} signals with PMA treatment is also consistent with the PKC-DR data, where negative feedback effects of PKC are ablated.

We also compared the effects of PMA, BIM, and PKC-DR on total [^{3}H]inositol phosphate accumulation (Fig. 7*E*). PKC-DR and acute BIM treatment both potentiated inositol phosphate accumulation in comparison with vasopressin alone. This corroborates our single-cell Ca^{2+} and IP_3 imaging data, indicating that elimination of PKC activity results in elevated IP_3 generation because of loss of negative feedback. At the single cell level, acute PMA treatment reduced Ca^{2+} oscillation frequency (Fig. 7*C*), but there was no comparable effect on [^{3}H]inositol phosphate accumulation (Fig. 7*E*). This finding may reflect multiple opposing effects of PKC, including negative regulation of PLC activation and positive regulation of IP_3 5-phosphatase (49), because the assay measures total inositol phosphate formation in the presence of Li^+. This assay was used because the low sensitivity of the [^{3}H]inositol labeling approach in hepatocytes precludes measurement of individual IP_3 isomers. Taken together, the data described above demonstrate that acute inhibition of PKC or PKC-DR eliminates an important negative feedback pathway at the level of hormone-stimulated PLC activity and/or IP_3 metabolism, leading to sustained or significantly broader Ca^{2+} transients. Consistent with this, acute activation of PKC blunts hormone-induced Ca^{2+} responses because of activation of these negative feedback loops. Therefore, PKC acts at multiple targets to modulate the frequency and shape of hormone-induced Ca^{2+} oscillations.

Effects of PKC on Ca^{2+} Oscillations Induced by Uncaging IP_3—To further elucidate targets of PKC, we examined the effect of PKC-DR and acute activation or inhibition of PKC on Ca^{2+} oscillations triggered by uncaging IP_3. Significantly, comparison of IP_3-induced Ca^{2+} transients in control 4α-PMA-treated cells and PKC-DR cells (representative traces are shown in Fig. 8*A*) revealed no differences in the Ca^{2+} signals elicited by increasing exposure to UV. PKC-DR had no effect on the proportion of cells responding (Fig. 8*B*) or the type of Ca^{2+} signature observed (Fig. 8*C*). Furthermore, no signifi-

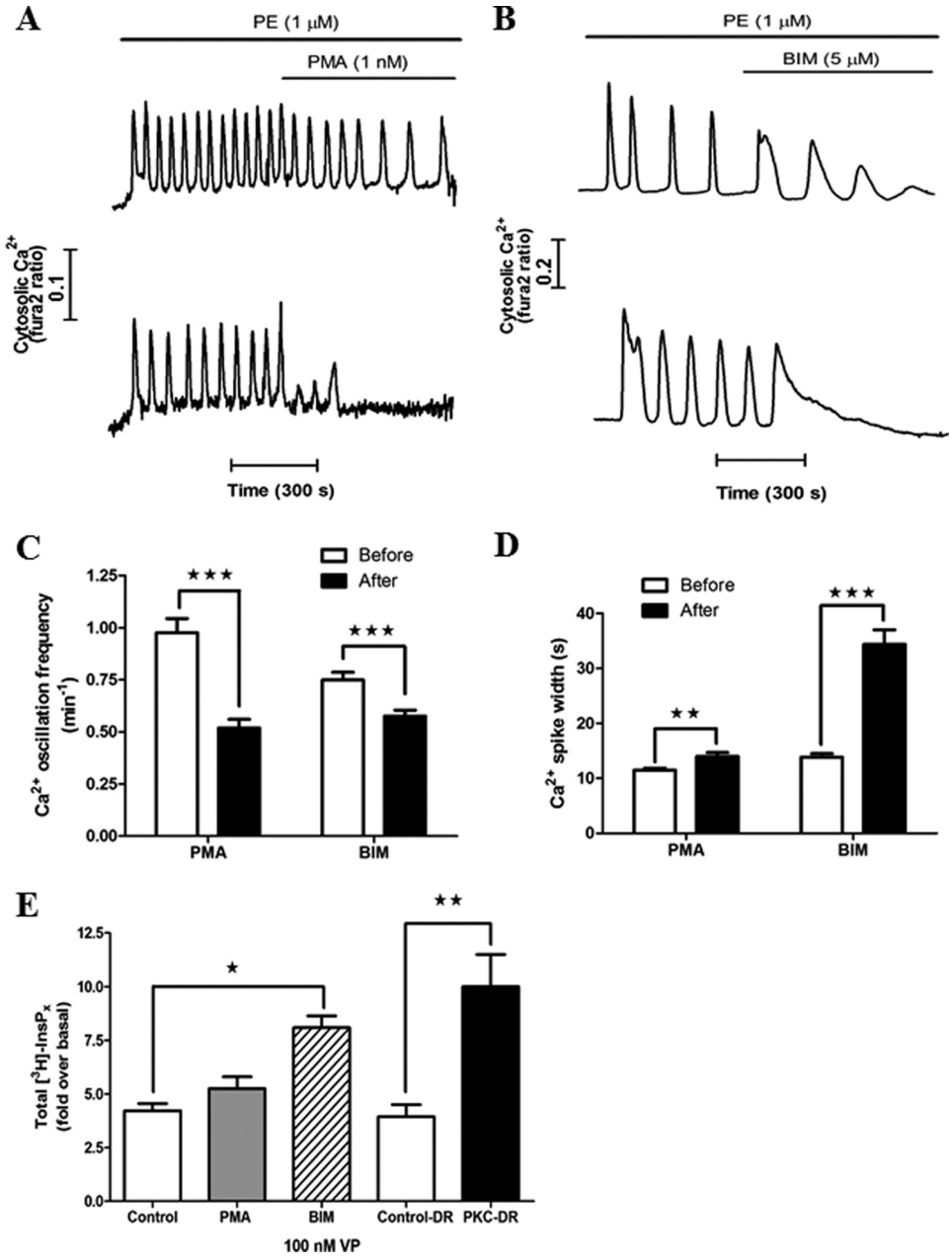

FIGURE 7. **Effects of acute activation and inhibition of PKC on hormone-induced Ca^{2+} oscillations.** The effects of PMA (1 nM) and BIM (5 μM) on phenylephrine (*PE*)-induced Ca^{2+} oscillations were examined in hepatocytes cultured for 1 h. Representative traces of PMA- (*A*) and BIM-treated (*B*) hepatocytes show either a decrease in oscillation frequency (*top panel*) or suppression of oscillations (*bottom panel*). The effect of drug treatment on phenylephrine-induced Ca^{2+} oscillation frequency (*C*) and Ca^{2+} spike width at half-peak height (*D*) are summarized. The frequencies of agonist-induced Ca^{2+} oscillations were calculated from 5-min periods in the absence or presence of the drugs. Ca^{2+} spike widths were calculated from the three oscillations prior to and after drug treatment. The drugs were present at least 1 min prior to carrying out the analysis. Data are mean ± S.E. from ≥15 cells from three independent experiments. **, $p < 0.01$; ***, $p < 0.001$; Student's *t* test. *E*, the effect of acute activation or inhibition of PKC and PKC-DR on total inositol phosphate production in response to 100 nM vasopressin (*VP*) stimulation for 15 min. Data are expressed as -fold increase over basal and are the mean ± S.E. from three independent experiments. *, $p < 0.05$; **, $p < 0.01$; analysis of variance.

cant effects were observed on Ca^{2+} oscillation frequency (Fig. 8*D*) or Ca^{2+} spike width (Fig. 8*E*). Therefore, elimination of phorbol ester-sensitive PKC activity through PKC down-regulation does not affect IP_3R function in the absence of hormone.

Acute treatment of cells with PMA or BIM (representative traces are shown in Fig. 8*F*) was also without effect on the proportion of cells responding to photorelease of caged IP_3 (Fig. 8*G*) or the Ca^{2+} spike width for oscillations resulting from IP_3 uncaging (data not shown). However, PKC activation with PMA causes a 2-fold increase in the Ca^{2+} oscillation frequency elicited by photo-released IP_3, from 1.1 ± 0.26 spikes min^{-1} in control cells to 2.35 ± 0.30 min^{-1} in PMA-treated cells (Fig. 8*H*). This is in clear contrast to the inhibitory effect of PMA to reduce the frequency of phenylephrine-induced Ca^{2+} oscillations (Fig. 7*C*). This result suggests that there is a direct modulation of IP_3Rs by PKC, which enhances channel activity and excitability. With global activation of PKC by PMA, the nega-

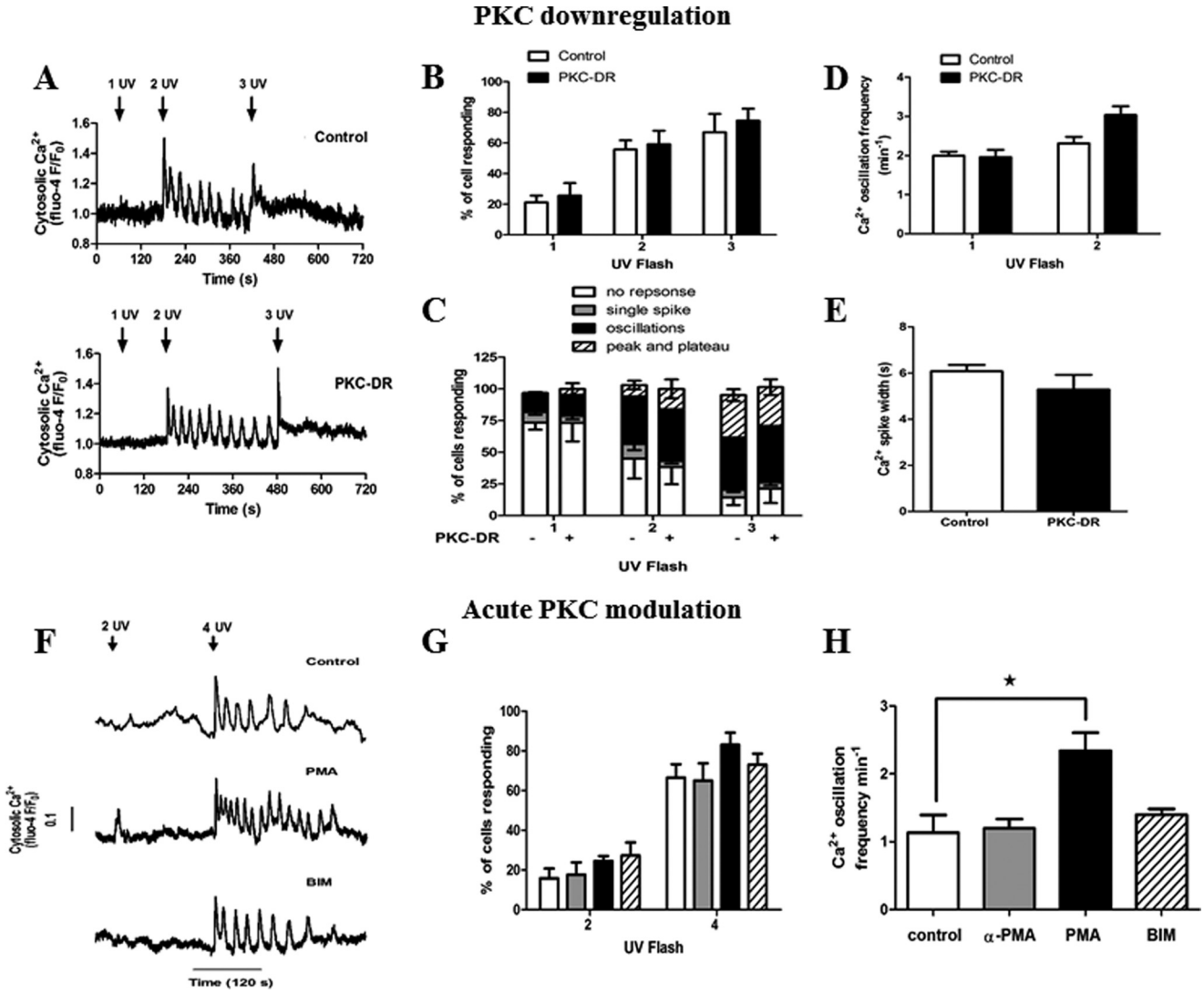

FIGURE 8. **Effects of PKC on IP_3 release-induced Ca^{2+} oscillations.** *A–E*, hepatocytes were treated overnight with 4α-PMA (1 μM, *Control*) or PMA (1 μM, *PKC-DR*) then loaded with caged IP_3 and Fluo-4. Shown are representative traces of single control and PKC-DR hepatocytes stimulated with increasing UV light flashes (*A*), the percentage of cells responding to one, two, and three UV light flashes (*B*), the percentage of cells with no response, single spike, oscillations, or saturated (peak/plateau) Ca^{2+} responses (*C*), the oscillation frequency (*D*), and the spike width half-peak height (*E*). *F—H*, overnight cultured hepatocytes loaded with caged IP_3 and Fluo-4 were treated with PMA (1 μM), 4α-PMA (1 μM), or BIM (5 μM) for 5 min prior to IP_3 uncaging (*F*) representative traces. Data summarize (*G*) the percentage of cells responding to two and four UV light flashes and (*H*) the oscillation frequency after four UV flashes. Data are mean ± S.E. from ≥25 cells from four independent experiments. *, $p < 0.05$, analysis of variance.

tive feedback mediated by PLC inhibition presumably predominates during hormone stimulation, whereas the positive feedback effect on IP_3-induced Ca^{2+} release becomes apparent during IP_3 uncaging when PLC is not activated. Therefore, under physiological conditions, activation of PKC by specific hormone receptors may differentially target negative feedback regulation of IP_3 generation (or degradation) and positive feedback on Ca^{2+} release to shape the resulting Ca^{2+} transients.

PKC Activity Modulates Ca^{2+} Wave Velocity in Response to Both Hormone and Photorelease of Caged IP_3—In the liver, hepatocyte and whole organ function is regulated not only by Ca^{2+} spike frequency but by Ca^{2+} wave propagation across individual cells (intracellular waves) and between cells (intercellular waves) within the liver lobule (5, 50–52). The propagation rates for hormone-induced intracellular Ca^{2+} waves are fixed over a wide range of agonist doses (52, 53). This lack of dependence on stimulus strength has led to the assumption that Ca^{2+} wave propagation is driven by a saltatory CICR processes (5, 54). However, we reported recently that the cytosolic expression of an intracellular IP_3 buffer slows Ca^{2+} wave velocity in a stimulus strength-dependent fashion (20). Those findings are consistent with a role for regeneration of IP_3 via positive feedback of Ca^{2+} on PLC, either globally or locally, which yields a cross-coupling between IP_3 and Ca^{2+} that maximizes the CICR process, leading to stereotypic waves of IP_3R activation.

In this study, we examined whether PKC has the potential to regulate Ca^{2+} wave propagation rates in addition to Ca^{2+} oscillation frequency and kinetics. First we examined the effect of PKC activation and down-regulation on intracellular Ca^{2+} waves elicited by IP_3 uncaging. As shown in Fig. 9*A*, acute activation of PKC with PMA led to a 2-fold increase in the rates of Ca^{2+} waves elicited by photorelease of IP_3 (16 ± 3.8 μm/s in control 4α-PMA treated cells *versus* 35.5 ± 5.4 μm/s after PMA treatment). This enhancement of Ca^{2+} wave propagation likely

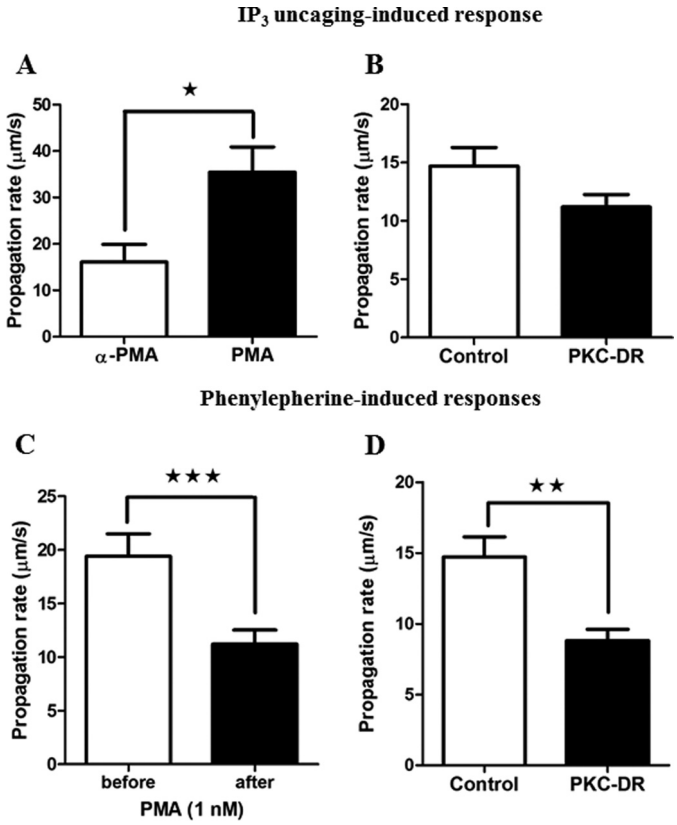

FIGURE 9. **Ca^{2+} wave velocity is regulated by PKC activity.** Isolated hepatocytes were treated overnight with 4α-PMA (1 μM, *Control*) or PMA (1 μM, *PKC-DR*) or treated acutely with 1 nM PMA to assess the effect of PKC on Ca^{2+} waves initiated by phenylephrine or caged IP_3. Ca^{2+} wave propagation rates were calculated in micrometers per second by determining time at half-peak height from regions of interest from the wave initiation site and the opposite pole of the hepatocyte. *A* and *B*, the effect of acute PKC activation (1 μM PMA, *A*) and PKC-DR down-regulation (*B*) on caged IP_3 (three UV flashes) induced Ca^{2+} wave velocity (micrometers per second ± S.E. for ≥16 cells from three independent experiments). *C* and *D*, the effect of acute PKC activation (1 nM) (*C*) and PKC-DR (*D*) on Ca^{2+} wave propagation rate in response to phenylephrine. Data are mean wave velocity (micrometers per second) ± S.E. for ≥18 cells from four independent experiments and from ≥20 cells from three independent experiments, respectively. *, $p < 0.05$; **, $p < 0.01$; ***, $p < 0.001$; Student's *t* test.

reflects the potentiation of IP_3R activity that also manifests as an increased Ca^{2+} oscillation frequency during IP_3 uncaging (Fig. 8*F*). As with IP_3-induced Ca^{2+} oscillations, the effect of PKC down-regulation on Ca^{2+} wave propagation was not significant (Fig. 9*B*), presumably because there is little basal activity even without PKC-DR in the absence of hormone stimulation.

The effect of PKC on hormone-induced Ca^{2+} waves is more complex because it affects both IP_3 generation and IP_3R function. In phenylephrine-stimulated hepatocytes, acute activation of PKC with PMA caused a decrease in Ca^{2+} wave velocity from a control rate of 19.4 ± 2.0 μm/s to 11.2 ± 1.3 μm/s (Fig. 9*C*). The negative effect of acute PMA on Ca^{2+} wave velocity presumably results from suppression of IP_3 production via enhanced negative feedback inhibition at the level of the hormone receptor or PLC. Therefore, the inhibitory effect of PMA predominates just as it does for the generation of Ca^{2+} oscillations (Fig. 7). However, despite the fact that PKC-DR prevents this inhibitory effect on PLC activation and greatly enhances IP_3 generation, its predominant effect at the level of Ca^{2+} waves was also to slow the rate of propagation. The wave propagation rate in control 4α-PMA treated cells was 14.7 ± 1.4 μm/s, and this decreased to 8.8 ± 0.8 μm/s after PKC down-regulation (Fig. 9*D*). Therefore, in the presence of hormone, the effects of PKC-DR are also manifest in a reduced level of IP_3R excitability. This provides further evidence that hormone-activated PKC positively regulates Ca^{2+} release and wave propagation by enhancing IP_3R function, either directly or indirectly. Taken together, these data demonstrate that PKC activation during hormone stimulation of the GPCR/PLC signaling system has positive (targeting the IP_3R) and negative feedback (IP_3 generation and metabolism) mechanisms that regulate Ca^{2+} spike width, oscillation frequency, and wave velocity.

Discussion

IP_3-dependent Ca^{2+} oscillations and waves are a major class of Ca^{2+} signals, and understanding the mechanisms that drive the oscillatory behavior and shape the kinetics of individual Ca^{2+} spikes is key to elucidating how Ca^{2+}-regulated targets are modulated. There is a substantial stochastic component to IP_3R-dependent Ca^{2+} oscillations (55), but the Ca^{2+} responses to different hormones have distinct stereotypic shapes with hormone-specific kinetic properties in hepatocytes (1, 34). Therefore, there must be further deterministic regulation of the Ca^{2+} signaling machinery beyond IP_3R isoform expression and subcellular distribution. A combination of modeling and experimental data demonstrate that hormone-induced Ca^{2+} oscillations in hepatocytes depend on positive feedback of Ca^{2+} on PLC and consequent cross-coupling of Ca^{2+} and IP_3 oscillations (17, 20).

In this study, we characterized Ca^{2+} responses induced by IP_3 uncaging in hepatocytes and show that, in the absence of a GPCR ligand, Ca^{2+} oscillations are driven by CICR and do not require PLC activation. This is on the basis of a number of lines of evidence. First, PLC inhibition failed to suppress Ca^{2+} oscillations elicited by direct release of IP_3. Second, graded steps of IP_3 uncaging with increasing numbers of UV flashes in the absence of hormone resulted in stimulus strength-dependent effects on Ca^{2+} spike amplitude, width, and wave velocity. This is in clear contrast to the constant Ca^{2+} spike amplitude and kinetic properties for GPCR-dependent Ca^{2+} oscillations and waves over a wide range of hormone doses (1, 5, 6, 9, 56). Third, Ca^{2+} spike widths elicited by caged IP_3 were of substantially shorter duration than hormone-induced Ca^{2+} oscillations reported in this study and previously (1, 9). Significantly, these data demonstrate that, although Ca^{2+} oscillations can be generated by CICR at the IP_3R independent of PLC activity, this is not sufficient to recapitulate the oscillatory Ca^{2+} signals elicited by hormones. Regenerative PLC activation and cyclical fluctuations in IP_3 levels are essential features of hormone-generated baseline-separated Ca^{2+} oscillations. The ability to compare IP_3 uncaging with GPCR-generated Ca^{2+} signals has enabled us to further dissect how Ca^{2+} oscillations are shaped and regulated.

It has been suggested that hormone-induced Ca^{2+} oscillations may rely in part on positive Ca^{2+} feedback regulation of the Ca^{2+} sensitive, but hormone-insensitive, PLC isoforms, *i.e.*

δ and η (57, 58). However, we found that global Ca^{2+} increases induced by photolysis of caged IP_3 do not increase PLC activity in hepatocytes, even though this causes similar $[Ca^{2+}]_i$ increases to those observed with hormone, in a range (0.1–10 μM) sufficient to activate PLCδ isoforms (59). On the basis of these data, we conclude that GPCR stimulation is a prerequisite for regenerative PLC activation and, presumably, depends on the PLCβ isoforms.

We found that photorelease of IP_3 caused Ca^{2+} oscillations with similar frequency in the presence or absence of extracellular Ca^{2+}. This provides evidence that plasma membrane Ca^{2+} entry pathways and the associated refilling of intracellular Ca^{2+} stores is not an intrinsic component of IP_3-dependent Ca^{2+} oscillations in hepatocytes (39). In addition, these data suggest that the Ca^{2+} filling state of the ER does not determine Ca^{2+} oscillation frequency in hepatocytes. Nevertheless, we observed a reduction in Ca^{2+} spike width in the absence of Ca^{2+} entry, providing evidence that store-operated Ca^{2+} entry can play a role in shaping Ca^{2+} transients.

PKC isoenzymes are key mediators of GPCR/PLC signaling, acting to decode complex spatiotemporal Ca^{2+} changes and regulate cell function (31, 32). However, because many of the proteins involved in generating Ca^{2+} signals are also PKC substrates, this family of enzymes may also dynamically regulate Ca^{2+} signaling (25, 29). Indeed, multiple and sometimes opposing effects of PKC on PLC, IP_3, and Ca^{2+} release are highlighted in this study, revealing targets both upstream and downstream of IP_3 generation. Down-regulation of phorbol ester-sensitive PKC isoforms had the most dramatic effect on the hormone-induced Ca^{2+} oscillations, potentiating PLC activity and the intracellular levels of IP_3 and Ca^{2+}.

The effects of acute PKC inhibition with BIM were similar to PKC-DR, evoking broader Ca^{2+} spike widths and maximal Ca^{2+} responses in the presence of hormone. By contrast, inhibition or elimination of PKC activity had no effect on the Ca^{2+} responses elicited by direct photorelease of caged IP_3. These data demonstrate a fundamental role of PKC in the termination of Ca^{2+} transients via negative feedback regulation of IP_3 levels. Indeed, differences in the declining phase of each Ca^{2+} spike during Ca^{2+} oscillations elicited by activation of distinct GPCRs (1, 6) may reflect differential sensitivity to PKC or specific pools of PKC associated with each hormone receptor type (61).

The effects of acute PKC activation were more complex. PMA treatment modestly decreased Ca^{2+} oscillation frequency and spike width in the presence of hormone, whereas the frequency of oscillations after direct release of IP_3 was increased. These data can be explained by dual opposing actions of PKC to suppress IP_3 generation while enhancing IP_3R activity. Most interesting is our observation that PKC down-regulation decreases Ca^{2+} wave velocity in the presence of hormone, despite increasing IP_3 generation. Although these results may appear contradictory, they can also be explained by the dual actions of PKC to inhibit IP_3 generation and enhance IP_3-induced Ca^{2+} release. Specifically, even though PKC-DR suppresses the negative feedbacks that limit IP_3 generation, allowing for more prolonged Ca^{2+} release in response to hormone, PKC-DR also eliminates the positive actions of PKC to enhance IP_3R excitability and, thereby, slows Ca^{2+} wave propagation. This is supported by the very different effects of PKC-DR and PMA on the velocity of Ca^{2+} waves initiated by photorelease of caged IP_3. Therefore, PKC-DR has no effect on IP_3-induced Ca^{2+} waves because there is no role for negative feedback of PKC on IP_3 generation and no sensitization of the IP_3R (this would require PLC activation and diacylglycerol generation). Similarly, PMA dramatically enhances IP_3-induced Ca^{2+} waves because it directly sensitizes the IP_3R but has no negative feedback effect on IP_3 generation. This modulation of Ca^{2+} wave propagation rates by PKC action on IP_3R sensitivity provides an important, hitherto unrecognized, level of regulation of intracellular Ca^{2+} signaling.

Taken together, the data presented here show that PKC regulates multiple and sometimes counteracting steps in the IP_3-dependent Ca^{2+} signaling pathway. Our data identify a number of potential PKC targets capable of Ca^{2+} signal modulation, but further work is required to elucidate which PKC isoforms regulate each target and whether these are cell type/receptor-specific. Translocation of GFP-tagged PKC isoenzymes have provided some insight into receptor-specific effects (62) or differential subcellular distributions of the enzymes upon hormone stimulation (60). However, whether the endogenous PKCs behave in a similar fashion or whether overexpressed PKC protein buffers cellular responses leave the data open to interpretation.

We conclude that, in the presence of sufficient cytosolic IP_3, Ca^{2+} oscillations and waves can be generated in hepatocytes simply by biphasic regulation of the IP_3R by Ca^{2+}. However, at physiologically relevant hormone levels, Ca^{2+} oscillations depend on positive feedback of Ca^{2+} on PLCβ and are driven by cross-coupling between Ca^{2+} and IP_3, and these elements of the Ca^{2+} signaling pathway can be specifically tuned and modulated by PKC. Therefore, physiological activation and deactivation of different PKC isoforms with distinct temporal and spatial profiles has the ability to profoundly shape Ca^{2+} oscillation kinetics, wave propagation rates, and the balance between positive and negative feedback mechanisms.

Author Contributions—A. P. T., P. J. B., and L. D. G. conceived and designed the study. P. J. B. wrote the manuscript. P. J. B. and W. M. designed and performed experiments and analyzed data. All authors reviewed the results and approved the final version of the manuscript.

References

1. Rooney, T. A., Sass, E. J., and Thomas, A. P. (1989) Characterization of cytosolic calcium oscillations induced by phenylephrine and vasopressin in single fura-2-loaded hepatocytes. *J. Biol. Chem.* **264,** 17131–17141
2. Bootman, M. D., Berridge, M. J., and Lipp, P. (1997) Cooking with calcium: the recipes for composing global signals from elementary events. *Cell* **91,** 367–373
3. Berridge, M. J., Lipp, P., and Bootman, M. D. (2000) The versatility and universality of calcium signalling. *Nat. Rev. Mol. Cell Biol.* **1,** 11–21
4. Thomas, A. P., Renard, D. C., and Rooney, T. A. (1991) Spatial and temporal organization of calcium signalling in hepatocytes. *Cell Calcium* **12,** 111–126
5. Gaspers, L. D., and Thomas, A. P. (2005) Calcium signaling in liver. *Cell Calcium* **38,** 329–342

6. Bartlett, P. J., Gaspers, L. D., Pierobon, N., and Thomas, A. P. (2014) Calcium-dependent regulation of glucose homeostasis in the liver. *Cell Calcium* **55,** 306–316
7. Irvine, R. F. (2003) 20 years of Ins(1,4,5)P3, and 40 years before. *Nat. Rev. Mol. Cell Biol.* **4,** 580–585
8. Bootman, M. D., Young, K. W., Young, J. M., Moreton, R. B., and Berridge, M. J. (1996) Extracellular calcium concentration controls the frequency of intracellular calcium spiking independently of inositol 1,4,5-trisphosphate production in HeLa cells. *Biochem. J.* **314,** 347–354
9. Thomas, A. P., Bird, G. S., Hajnóczky, G., Robb-Gaspers, L. D., and Putney, J. W., Jr. (1996) Spatial and temporal aspects of cellular calcium signaling. *FASEB J.* **10,** 1505–1517
10. Dupont, G., Combettes, L., Bird, G. S., and Putney, J. W. (2011) Calcium oscillations. *Cold Spring Harb. Perspect. Biol.* **3,**
11. Sneyd, J., Tsaneva-Atanasova, K., Reznikov, V., Bai, Y., Sanderson, M. J., and Yule, D. I. (2006) A method for determining the dependence of calcium oscillations on inositol trisphosphate oscillations. *Proc. Natl. Acad. Sci. U.S.A.* **103,** 1675–1680
12. Meyer, T., and Stryer, L. (1988) Molecular model for receptor-stimulated calcium spiking. *Proc. Natl. Acad. Sci. U.S.A.* **85,** 5051–5055
13. Bezprozvanny, I., Watras, J., and Ehrlich, B. E. (1991) Bell-shaped calcium-response curves of Ins(l,4,5)P3- and calcium-gated channels from endoplasmic reticulum of cerebellum. *Nature* **351,** 751–754
14. Thurley, K., and Falcke, M. (2011) Derivation of Ca^{2+} signals from puff properties reveals that pathway function is robust against cell variability but sensitive for control. *Proc. Natl. Acad. Sci. U.S.A.* **108,** 427–432
15. De Young, G. W., and Keizer, J. (1992) A single-pool inositol 1,4,5-trisphosphate-receptor-based model for agonist-stimulated oscillations in Ca^{2+} concentration. *Proc. Natl. Acad. Sci. U.S.A.* **89,** 9895–9899
16. Marchant, J. S., and Parker, I. (2001) Role of elementary $Ca(^{2+})$ puffs in generating repetitive $Ca(^{2+})$ oscillations. *EMBO J.* **20,** 65–76
17. Politi, A., Gaspers, L. D., Thomas, A. P., and Höfer, T. (2006) Models of IP3 and Ca^{2+} oscillations: frequency encoding and identification of underlying feedbacks. *Biophys. J.* **90,** 3120–3133
18. Salazar, C., Politi, A. Z., and Höfer, T. (2008) Decoding of calcium oscillations by phosphorylation cycles: analytic results. *Biophys. J.* **94,** 1203–1215
19. Dupont, G., and Erneux, C. (1997) Simulations of the effects of inositol 1,4,5-trisphosphate 3-kinase and 5-phosphatase activities on Ca^{2+} oscillations. *Cell Calcium* **22,** 321–331
20. Gaspers, L. D., Bartlett, P. J., Politi, A., Burnett, P., Metzger, W., Johnston, J., Joseph, S. K., Höfer, T., and Thomas, A. P. (2014) Hormone-induced calcium oscillations depend on cross-coupling with inositol 1,4,5-trisphosphate oscillations. *Cell Rep.* **9,** 1209–1218
21. Dolmetsch, R. E., Xu, K., and Lewis, R. S. (1998) Calcium oscillations increase the efficiency and specificity of gene expression. *Nature* **392,** 933–936
22. Li, W., Llopis, J., Whitney, M., Zlokarnik, G., and Tsien, R. Y. (1998) Cell-permeant caged InsP3 ester shows that Ca^{2+} spike frequency can optimize gene expression. *Nature* **392,** 936–941
23. Zhu, L., Song, S., Pi, Y., Yu, Y., She, W., Ye, H., Su, Y., and Hu, Q. (2011) Cumulated Ca^{2+} spike duration underlies Ca^{2+} oscillation frequency-regulated NFκB transcriptional activity. *J. Cell Sci.* **124,** 2591–2601
24. Newton, A. C. (2001) Protein kinase C: structural and spatial regulation by phosphorylation, cofactors, and macromolecular interactions. *Chem. Rev.* **101,** 2353–2364
25. Nash, M. S., Young, K. W., Challiss, R. A., and Nahorski, S. R. (2001) Intracellular signalling. Receptor-specific messenger oscillations. *Nature* **413,** 381–382
26. Young, K. W., Nash, M. S., Challiss, R. A., and Nahorski, S. R. (2003) Role of Ca^{2+} feedback on single cell inositol 1,4,5-trisphosphate oscillations mediated by G-protein-coupled receptors. *J. Biol. Chem.* **278,** 20753–20760
27. Strassheim, D., and Williams, C. L. (2000) P2Y2 purinergic and M3 muscarinic acetylcholine receptors activate different phospholipase C-β isoforms that are uniquely susceptible to protein kinase C-dependent phosphorylation and inactivation. *J. Biol. Chem.* **275,** 39767–39772
28. Foskett, J. K., White, C., Cheung, K.-H., and Mak, D.-O. D. (2007) Inositol trisphosphate receptor Ca^{2+} release channels. *Physiol. Rev.* **87,** 593–658
29. Vanderheyden, V., Devogelaere, B., Missiaen, L., De Smedt, H., Bultynck, G., and Parys, J. B. (2009) Regulation of inositol 1,4,5-trisphosphate-induced Ca^{2+} release by reversible phosphorylation and dephosphorylation. *Biochim. Biophys. Acta* **1793,** 959–970
30. Woodring, P. J., and Garrison, J. C. (1997) Expression, purification, and regulation of two isoforms of the inositol 1,4,5-trisphosphate 3-kinase. *J. Biol. Chem.* **272,** 30447–30454
31. Bartlett, P. J., Young, K. W., Nahorski, S. R., and Challiss, R. A. (2005) Single cell analysis and temporal profiling of agonist-mediated inositol 1,4,5-trisphosphate, Ca^{2+}, diacylglycerol, and protein kinase C signaling using fluorescent biosensors. *J. Biol. Chem.* **280,** 21837–21846
32. Oancea, E., and Meyer, T. (1998) Protein kinase C as a molecular machine for decoding calcium and diacylglycerol signals. *Cell* **95,** 307–318
33. Berrie, C. P., and Cobbold, P. H. (1995) Both activators and inhibitors of protein kinase C promote the inhibition of phenylephrine-induced $[Ca^{2+}]$i oscillations in single intact rat hepatocytes. *Cell Calcium* **18,** 232–244
34. Sanchez-Bueno, A., Dixon, C. J., Woods, N. M., Cuthbertson, K. S., and Cobbold, P. H. (1990) Inhibitors of protein kinase C prolong the falling phase of each free-calcium transient in a hormone-stimulated hepatocyte. *Biochem. J.* **268,** 627–632
35. Hajnóczky, G., and Thomas, A. P. (1997) Minimal requirements for calcium oscillations driven by the IP3 receptor. *EMBO J.* **16,** 3533–3543
36. Mikoshiba, K. (2007) IP3 receptor/Ca^{2+} channel: from discovery to new signaling concepts. *J. Neurochem.* **102,** 1426–1446
37. Dakin, K., and Li, W.-H. (2007) Cell membrane permeable esters of D-myo-inositol 1,4,5-trisphosphate. *Cell Calcium.* **42,** 291–301
38. Rooney, T. A., and Thomas, A. P. (1991) Organization of intracellular calcium signals generated by inositol lipid-dependent hormones. *Pharmacol. Ther.* **49,** 223–237
39. Smyth, J. T., Hwang, S. Y., Tomita, T., DeHaven, W. I., Mercer, J. C., and Putney, J. W. (2010) Activation and regulation of store-operated calcium entry. *J. Cell. Mol. Med.* **14,** 2337–2349
40. Putney, J. W., and Bird, G. S. (2008) Cytoplasmic calcium oscillations and store-operated calcium influx. *J. Physiol.* **586,** 3055–3059
41. Yamasaki-Mann, M., and Parker, I. (2011) Enhanced ER Ca^{2+} store filling by overexpression of SERCA2b promotes IP3-evoked puffs. *Cell Calcium.* **50,** 36–41
42. Fraiman, D., and Dawson, S. P. (2004) A model of the IP3 receptor with a luminal calcium binding site: stochastic simulations and analysis. *Cell Calcium.* **35,** 403–413
43. Brini, M., and Carafoli, E. (2011) The plasma membrane Ca^{2+} ATPase and the plasma membrane sodium calcium exchanger cooperate in the regulation of cell calcium. *Cold Spring Harb. Perspect. Biol.* **3,** a004168
44. Kawasaki, T., Ueyama, T., Lange, I., Feske, S., and Saito, N. (2010) Protein kinase C-induced phosphorylation of Orai1 regulates the intracellular Ca^{2+} level via the store-operated Ca^{2+} channel. *J. Biol. Chem.* **285,** 25720–25730
45. Dupont, G., Lokenye, E. F., and Challiss, R. A. (2011) A model for Ca^{2+} oscillations stimulated by the type 5 metabotropic glutamate receptor: an unusual mechanism based on repetitive, reversible phosphorylation of the receptor. *Biochimie* **93,** 2132–2138
46. van der Wal, J., Habets, R., Várnai, P., Balla, T., and Jalink, K. (2001) Monitoring agonist-induced phospholipase C Activation in live cells by fluorescence resonance energy transfer. *J. Biol. Chem.* **276,** 15337–15344
47. Hajnóczky, G., Robb-Gaspers, L. D., Seitz, M. B., and Thomas, A. P. (1995) Decoding of cytosolic calcium oscillations in the mitochondria. *Cell* **82,** 415–424
48. Robb-Gaspers, L. D., Rutter, G. A., Burnett, P., Hajnóczky, G., Denton, R. M., and Thomas, A. P. (1998) Coupling between cytosolic and mitochondrial calcium oscillations: role in the regulation of hepatic metabolism. *Biochim. Biophys. Acta* **1366,** 17–32
49. Connolly, T. M., Lawing, W. J., Jr., and Majerus, P. W. (1986) Protein kinase C phosphorylates human platelet inositol trisphosphate 5′-phosphomonoesterase, increasing the phosphatase activity. *Cell* **46,** 951–958
50. Nathanson, M. H., Burgstahler, A. D., Mennone, A., Fallon, M. B., Gonzalez, C. B., and Saez, J. C. (1995) Ca^{2+} waves are organized among hepato-

cytes in the intact organ. *Am. J. Physiol. Gastrointest. Liver Physiol.* **269,** G167–G171
51. Tordjmann, T., Berthon, B., Jacquemin, E., Clair, C., Stelly, N., Guillon, G., Claret, M., and Combettes, L. (1998) Receptor-oriented intercellular calcium waves evoked by vasopressin in rat hepatocytes. *EMBO J.* **17,** 4695–4703
52. Robb-Gaspers, L. D., and Thomas, A. P. (1995) Coordination of Ca signaling by intercellular propagation of Ca waves in the intact liver. *J. Biol. Chem.* **270,** 8102–8107
53. Rooney, T. A., Sass, E. J., and Thomas, A. P. (1990) Agonist-induced cytosolic calcium oscillations originate from a specific locus in single hepatocytes. *J. Biol. Chem.* **265,** 10792–10796
54. Nathanson, M. H., Burgstahler, A. D., and Fallon, M. B. (1994) Multistep mechanism of polarized Ca^{2+} wave patterns in hepatocytes. *Am. J. Physiol. Gastrointest. Liver Physiol.* **267,** G338–G349
55. Thurley, K., Tovey, S. C., Moenke, G., Prince, V. L., Meena, A., Thomas, A. P., Skupin, A., Taylor, C. W., and Falcke, M. (2014) Reliable encoding of stimulus intensities within random sequences of intracellular Ca^{2+} spikes. *Sci. Signal.* **7,** ra59
56. Rooney, T. A., Renard, D. C., Sass, E. J., and Thomas, A. P. (1991) Oscillatory cytosolic calcium waves independent of stimulated inositol 1,4,5-trisphosphate formation in hepatocytes. *J. Biol. Chem.* **266,** 12272–12282
57. Banno, Y., Okano, Y., and Nozawa, Y. (1994) Thrombin-mediated phosphoinositide hydrolysis in Chinese hamster ovary cells overexpressing phospholipase C-δ 1. *J. Biol. Chem.* **269,** 15846–15852
58. Kim, J. K., Choi, J. W., Lim, S., Kwon, O., Seo, J. K., Ryu, S. H., and Suh, P.-G. (2011) Phospholipase C-η1 is activated by intracellular Ca^{2+} mobilization and enhances GPCRs/PLC/Ca^{2+} signaling. *Cell. Signal.* **23,** 1022–1029
59. Allen, V., Swigart, P., Cheung, R., Cockcroft, S., and Katan, M. (1997) Regulation of inositol lipid-specific phospholipase cδ by changes in Ca^{2+} ion concentrations. *Biochem. J.* **327,** 545–552
60. Collazos, A., Diouf, B., Guérineau, N. C., Quittau-Prévostel, C., Peter, M., Coudane, F., Hollande, F., and Joubert, D. (2006) A spatiotemporally coordinated cascade of protein kinase C activation controls isoform-selective translocation. *Mol. Cell. Biol.* **26,** 2247–2261
61. Shin, D. M., Luo, X., Wilkie, T. M., Miller, L. J., Peck, A. B., Humphreys-Beher, M. G., and Muallem, S. (2001) Polarized expression of G protein-coupled receptors and an all-or-none discharge of Ca^{2+} pools at initiation sites of [Ca^{2+}] i waves in polarized exocrine cells. *J. Biol. Chem.* **276,** 44146–44156
62. Uchino, M., Sakai, N., Kashiwagi, K., Shirai, Y., Shinohara, Y., Hirose, K., Iino, M., Yamamura, T., and Saito, N. (2004) Isoform-specific phosphorylation of metabotropic glutamate receptor 5 by protein kinase C (PKC) blocks Ca^{2+} oscillation and oscillatory translocation of Ca^{2+}-dependent PKC. *J. Biol. Chem.* **279,** 2254–2261